Optical heterodyne detection of laser-induced gratings

A. A. Maznev and K. A. Nelson

Department of Chemistry, Massachusetts Institute of Technology, Cambridge, Massachusetts 02139

J. A. Rogers

Lucent Technologies, Murray Hill, New Jersey 07974

Received May 8, 1998

A novel optical arrangement for heterodyne detection of laser-induced gratings based on the use of a phase mask for both excitation and probe beams provides phase stability and control without the need for an active stabilization scheme. The arrangement greatly simplifies the laser-induced grating experiment. The performance of the technique in both transmission and reflection geometries is illustrated through measurements of bulk and surface acoustic waves generated by picosecond laser pulses. © 1998 Optical Society of America

OCIS codes: 300.6310, 300.2570, 300.6500, 050.0050.

Laser-induced dynamic grating spectroscopy[1] is a powerful time-resolved optical technique that is widely used to study a broad range of phenomena such as molecular and lattice vibrations,[2] bulk and surface acoustic waves,[3–5] and relaxation and transport processes. In this technique, two interfering laser beams are crossed in the medium to produce spatially periodic material excitations that are monitored through diffraction of a third (probe) laser beam. The diffracted signal has the attractive feature of being background free in the sense that in the absence of excitation there is no diffraction of probe light. However, detection of small signals by this method is difficult because the diffraction efficiency is normally proportional to the square of the material excitation amplitude. Therefore the potential benefits of heterodyne detection that can be used to amplify the signal have long been recognized.[1]

In the heterodyne scheme, a fourth (local oscillator or reference) beam that is collinear with the diffracted probe beam is introduced. The coherent interference of reference and diffracted beams results in an output signal intensity given by

$$I_S = I_R + I_D + 2\sqrt{I_R I_D}\cos\theta\,, \tag{1}$$

where I_D and I_R are diffracted signal and reference intensities, respectively, and θ is the phase difference between their respective optical fields. For $I_R \gg I_D$ the signal of interest is given by the third term in Eq. (1) because the first term is constant and the second is negligibly small. Thus the signal is proportional to the square root of I_R, and one can increase it in magnitude simply by increasing the reference beam intensity. This procedure can help to overcome noise that is due to the detection electronics and, more importantly, to parasitically scattered light. Other advantages of heterodyne detection are signal linearity with respect to the material response amplitude and retention of phase information that would otherwise be lost.[6–8]

There are difficulties in practical implementation of the heterodyne detection technique. The phase difference θ must be stable, a condition that is normally ensured by an active stabilization scheme that uses a mirror mounted upon a piezoelectric transducer with a separate optical arrangement to provide feedback,[1,8,9] which may require a separate laser source.[8] In experiments with femtosecond time resolution[7,8] care must be taken to avoid a time delay between the probe and the reference pulses. Another practical problem is that the diffracted and reference beams should be strictly collinear to ensure the coincidence of their phase fronts; with weak diffraction levels, this requirement creates additional alignment challenges.

The difficulties mentioned above have severely limited the use of heterodyne detection in transient grating measurements. Although attempts have been made to find an alternative to the introduction of a reference beam, e.g., through heterodyning of the diffracted signal that arises from the material response of interest with additional diffraction from a thermal grating induced by the excitation pulses[6] or through heterodyning with light scattered parasitically from sample imperfections,[10] the need for a more widely applicable solution is obvious.

In this Letter we present a simple optical arrangement that makes optically heterodyned transient grating spectroscopy simple and attractive. The key feature of our optical arrangement, presented in Fig. 1, is the use of a diffraction grating (referred to below as a mask, to distinguish it from the laser-induced grating in the sample) to produce the excitation, probe, and reference beams, as suggested in Ref. 11. The mask is designed to optimize the diffraction efficiency

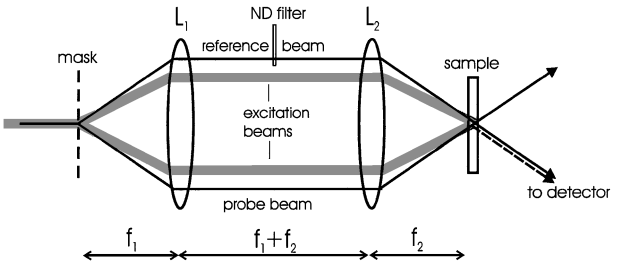

Fig. 1. Optical arrangement for heterodyne detection of laser-induced gratings in transmission geometry.

0146-9592/98/161319-03$15.00/0

of incident light into the first (± 1) diffraction orders. Upon diffraction of both excitation and probe beams by the mask pattern, first-order diffraction maxima are recombined by a telescope that images the mask pattern onto the sample, while all other diffraction orders are blocked by a spatial filter. As a result, there are the usual two excitation beams and also two (rather than the usual one) probe beams, of which one serves as the actual probe while the other is attenuated by a neutral-density filter and used as a reference beam.

Interference between the excitation pulses results in a periodic intensity pattern and associated material excitation grating characterized by the wavelength $\Lambda = M\Lambda_0/2$, where Λ_0 is the period of the phase mask and $M = f_2/f_1$ is the magnification ratio of the imaging system. Provided that the magnification M is the same at the excitation and the probe wavelengths, the probe and reference beams of wavelength λ_p always enter the sample at an angle φ_p that satisfies the Bragg diffraction condition, $\sin\varphi_p = \lambda_p/2\Lambda$. This characteristic by itself offers substantial advantages for alignment of transient grating experiments in thick samples where probe beam diffraction occurs in the Bragg regime. More important is the fact that the diffracted probe beam is automatically collinear with the reference beam; i.e., no additional alignment is needed for heterodyne detection. The excitation and probe beams are merely made collinear and overlap at the mask pattern. In fact, a finite angle can be introduced between the two beams incident upon the mask in the vertical plane perpendicular to the drawing, which yields a vertical separation of the signal from the transmitted excitation light. Thus the signal is spatially isolated, even if all the beams have the same wavelength and polarization. The beams then pass through the imaging system onto the sample, and the signal appears. Even quite a weak signal can be located by eye because it is collinear with the reference beam.

The relative phase stability of the diffracted and reference beams results from the fact that the excitation beams are produced by the same mask pattern as the reference and the probe. The optical phase of the diffracted probe beam depends on the spatial phase of the material excitation grating in the sample. The latter is determined by the phase difference between the excitation beams, which is equal to the phase difference between the probe and the reference beams. Consequently, the phase difference between the reference and diffracted probe beams is stable, and one can control it by varying the optical path length of the reference beam. The optical path can be varied by tilting the filter that attenuates the reference beam or through the use of a phase plate.

Thus we have a compact setup that greatly simplifies phase-stabilized heterodyne detection of laser-induced gratings. Additional benefits include simplicity in finding the signal, the absence of a delay between the excitation pulses, and automatic Bragg angle adjustment and the possibility to vary the grating period Λ easily by switching among mask patterns with different spacings. Note that, whereas Fig. 1 shows the laser-induced grating experiment in transmission geometry, the setup has also been used to detect laser-induced reflection gratings upon the surfaces of opaque materials.

In both transmission and reflection geometries, the frequency-doubled output of a mode-locked, Q-switched, and cavity-dumped Nd:YAG laser (pulse duration 100 ps, wavelength $\lambda_e = 532$ nm, energy 100 μJ) was used for excitation and an electro-optically gated beam from a cw argon-ion laser (pulse duration 10 μs, wavelength $\lambda_p = 514$ nm, cw power 0.5 W) was used as a probe. The excitation and probe beams, both vertically polarized, were focused onto the mask with spherical lenses (not shown in Fig. 1) of focal lengths 60 and 40 cm, respectively. To image the mask pattern onto the sample, we used spherical lenses with focal distances $f_1 = 25$ cm and $f_2 = 15$ cm. On the sample, the laser spot diameter was $\simeq$150 μm for the excitation pulses and $\simeq$100 μm for the probe and reference beams. The heterodyne signal was detected by a preamplified avalanche photodiode whose output was fed into an oscilloscope, with a 1-GHz overall bandwidth of the detection system.

The phase mask had a rectangular profile, introducing a periodic variation of the optical path length equal to $\lambda_e/2$. The mask diffracted $\simeq$75% of the energy into the two first (± 1) diffraction maxima at both 532 and 514 nm. The mask spacing was 20.5 μm, resulting in the grating period on the sample of $\Lambda = 6.15$ μm.

Figure 2(a) shows the signal obtained in the reflection geometry with or without heterodyning (i.e., with the reference beam open or blocked) from a 0.7-μm-thick nickel film on silicon. Optical absorption of the excitation pulses gives rise to sudden thermal expansion at the grating peaks, which launches counterpropagating surface acoustic waves (SAW's) of wavelength Λ that form a standing wave within the excitation region. The acoustic and thermal responses produce a spatially periodic modulation (ripple) on the sample surface, which acts as a grating and diffracts the probe light. The signal includes fast (570-MHz) SAW oscillations, slow oscillations that are due to acoustic waves in the air, and a slowly decaying thermal grating contribution.[5] As expected, the polarity of the heterodyne signal depends on the phase difference between the diffracted signal and the reference beam. The data shown represent averages over 1000 repetitive measurements. The phase stability was good, with no visible fluctuations observed during the course of the experiment.

Heterodyne detection not only results in an increase in the signal intensity but also provides additional information because of its phase sensitivity. This fact is illustrated well through observation of acoustic oscillations in a traveling SAW detected with the probe and reference beams moved away from the excitation spot. Heterodyne data that correspond to various distances between the excitation and probe beams are shown in Fig. 2(b). A diffraction signal without the reference beam reveals only the envelope of the traveling wave, with no time-dependent oscillations observed. Note that outside the excitation region we observed only a SAW signal without contributions from the thermal grating (which does not propagate) or

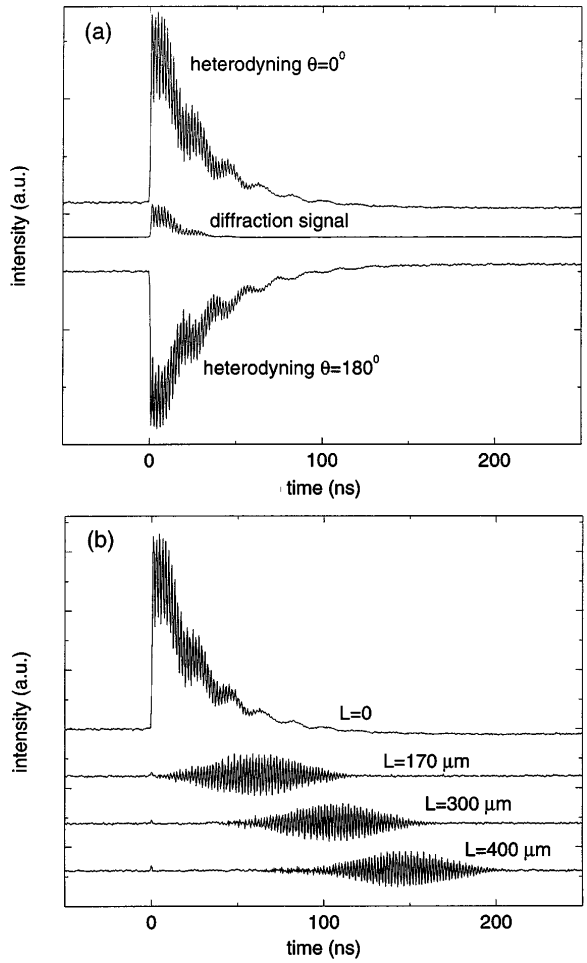

Fig. 2. Reflection mode measurements on a 0.7-μm-thick nickel film on silicon. (a) Diffraction signal (with the reference beam blocked) and heterodyne signals with phase differences between the probe and the reference beams of 0° and 180°. (b) Heterodyne signals obtained with various distances L between the excitation and the probe beams on the sample.

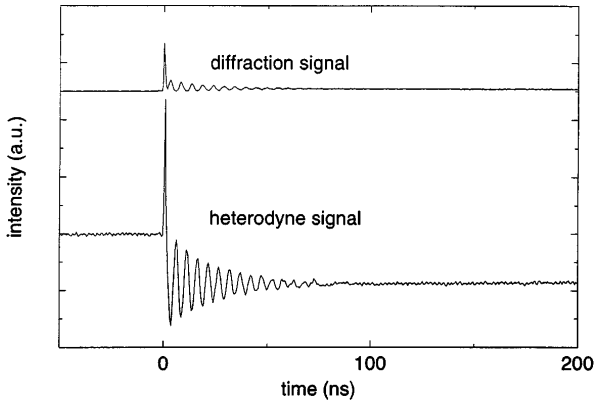

Fig. 3. Diffraction signal without heterodyning and heterodyne signal obtained in transmission mode from a 1 mm-thick liquid CS_2 sample.

acoustic waves in the air (which do not propagate far because of strong damping).

Another example of heterodyne detection is given by Fig. 3, which shows signals observed from liquid carbon disulfide in the transmission geometry. This measurement was performed in the Bragg diffraction regime and took advantage of the setting of the probe beam to the Bragg angle by the phase mask. Here, besides acoustic oscillations (in this case they are due to bulk longitudinal acoustic waves) and a thermal grating, we observe a peak at $t \simeq 0$ that is due to the nonlinear polarizability $\chi^{(3)}_{1111}$ that originates from both nonresonant electronic and molecular orientational motion responses.[12] In the heterodyne data the sign of the $\chi^{(3)}$ contribution is opposite that of the thermal grating. This is so because at the grating peaks (i.e., the excitation interference maxima) the thermal grating that is due to thermal expansion of heated material yields minima of the density and refractive index, whereas the $\chi^{(3)}$ grating yields maxima of the refractive index, in accordance with the positive sign of $\chi^{(3)}_{1111}$.[8]

In conclusion, the optical arrangement considered here offers an effective solution for phase-controlled heterodyne detection of laser-induced gratings. Considering the great simplification in the experimental setup and alignment as well as in the signal enhancement, this arrangement will be beneficial not only for acoustic measurements but for virtually any laser-induced dynamic grating experiment. In addition, the enhancements in information content that follow from the phase sensitivity of the technique offer new important capabilities such as independent determination of real and imaginary contributions to the material response.

The authors appreciate stimulating discussions with T. F. Crimmins. This research was supported by National Science Foundation grant DMR-9710140.

References

1. H. J. Eichler, P. Günter, and D. W. Pohl, *Laser-Induced Dynamic Gratings* (Springer-Verlag, Berlin, 1986).
2. L. Dhar, J. A. Rogers, and K. A. Nelson, Chem. Rev. **94,** 157 (1994).
3. M. D. Fayer, IEEE J. Quantum Electron. **QE-22,** 1437 (1986).
4. T. Sawada and A. Harata, Appl. Phys. A **61,** 263 (1995).
5. A. R. Duggal, J. A. Rogers, and K. A. Nelson, J. Appl. Phys. **72,** 2823 (1992); J. A. Rogers and K. A. Nelson, J. Appl. Phys. **75,** 1534 (1994).
6. P. Vöhringer and N. F. Scherer, J. Phys. Chem. **99,** 2684 (1995).
7. Y. J. Chang, P. Cong, and J. D. Simon, J. Phys. Chem. **99,** 7858 (1995).
8. S. Matsuo and T. Tahara, Chem. Phys. Lett. **264,** 636 (1997).
9. D. W. Pohl, IBM J. Res. Dev. **23,** 604 (1979).
10. H. J. Bakker, S. Hunshe, and H. Kurz, Phys. Rev. Lett. **69,** 2823 (1992).
11. J. A. Rogers, M. Fuchs, M. J. Banet, J. B. Hanselman, R. Logan, and K. A. Nelson, Appl. Phys. Lett. **71,** 225 (1997).
12. S. Ruhman, L. R. Williams, A. G. Joly, B. Kohler, and K. A. Nelson, J. Phys. Chem. **91,** 2237 (1987).